The Cryosphere Discuss., 8, 769–804, 2014
www.the-cryosphere-discuss.net/8/769/2014/
doi:10.5194/tcd-8-769-2014

The Cryosphere
Discussions
Open Access

Dating of a Dome Fuji (Antarctica) shallow ice core by volcanic signal synchronization with B32 and EDML1 chronologies

Y. Motizuki[1], Y. Nakai[1], K. Takahashi[1], M. Igarashi[2,*], H. Motoyama[2], and K. Suzuki[3]

[1]RIKEN Nishina Center, Hirosawa 2-1, Wako, Japan
[2]National Institute of Polar Research, Research Organization of Information and Systems, Midoricho 10-3, Tachikawa, Tokyo, Japan
[3]Department of Environmental Sciences, Shinshu University, Asahi 3-1-1, Matsumoto, Japan
[*]now at: Maruzen Co. Ltd., Tokyo, Japan

Received: 1 October 2013 – Accepted: 10 December 2013 – Published: 27 January 2014

Correspondence to: Y. Motizuki (motizuki@riken.jp)

Published by Copernicus Publications on behalf of the European Geosciences Union.

Abstract

We found extremely good synchronization of volcanic eruption signals between a shallow ice core drilled at Dome Fuji in 2001 (DF01 core) and the B32 shallow ice core from Dronning Maud Land, East Antarctica. We then applied volcanic signature matching to transfer the B32 chronology constructed by annual layer counting to a portion of the DF01 core for which annual layer counting was difficult because of the low precipitation rate. Matching was done by careful comparison of non-sea-salt sulfate (nssSO_4^{2-}) data, which have a temporal resolution of about 1 yr, between the DF01 and B32 cores. The newly obtained chronology is called DFS1 (Dome Fuji Shallow ice core 1). In total, 31 volcanic eruptions were synchronized from AD 1900 back to AD 187, the earliest volcanic eruption date in the B32 core. The mean accumulation rate between synchronized volcanic horizons of the Dome Fuji core relative to rates at the B32 core drilling site did not differ significantly between these dates, increasing our confidence in this matching approach. We also used the B32-correlated EDML1/EDC3 chronology obtained from the top part of the EPICA Dronning Maud Land (DML) deep ice core to date a portion of the DF01 core. This new chronology, called DFS2 (Dome Fuji Shallow ice core 2), uses the correlations between B32 and EDML1/EDC3 ages to date the DF01 core from AD 1900 back to AD 199; moreover, four volcanic eruption dates from the EDML1/EDC3 chronology were used to date the interval from AD 199 back to AD 1. Because the EDML1/EDC3 ages were determined by adopting the B32 chronology back to AD 1170, DFS1 and DFS2 dates are identical between AD 1170 and 1900. These two methods enabled us to obtain a detailed chronology of the DF01 core, in particular the part before the last millennium, which has been difficult before this. We also present the absolute mean accumulation rates at Dome Fuji between AD 1 and 1900, based on the DFS1 and DFS2 chronologies.

1 Introduction

The physical and chemical properties of ice cores from polar regions record paleoclimate and glaciological information. Although it is obvious that it is important to study deep ice cores containing records going back hundreds of thousands of years, it is also extremely valuable to analyze shallow ice cores with high temporal resolution to obtain information about the terrestrial environment during the last few thousand years. The main reason for this is that we have historical records on nature dating back to about the last two millennia, and modern observational data are available especially since the last century; by comparing these records directly with information on the terrestrial environment extracted from ice cores, we can use the understanding gained to extend our knowledge further into the past. Here, it is necessary to know the age of the ice as a function of depth, and the precision and accuracy of the ice core dates becomes crucial.

Provided that the accumulation rate is sufficiently high, it is possible to date a core by counting annual layers using seasonal variations observed in chemical species (e.g., Na^+, Cl^-, Mg^{2+}, nssSO_4^{2-}, $CH_3SO_3^-$(MSA), NO_3^-), stable isotope ratios ($\delta^{18}O$, δD), electric conductivity measurement (ECM), and/or visual stratigraphy (e.g., Sigl et al., 2013; Ferris et al., 2011; Vinther et al., 2006; Taylor et al., 2004; Traufetter et al., 2004; Budner and Cole-Dai, 2003; Kohno and Fujii, 2002; Fujii et al., 2001; Palmer et al., 2001; Sommer et al., 2000a). The annual layer counting is usually tuned by using stratigraphical tie points. For example, well-dated volcanic eruptions, specific features in the ^{10}Be concentration profile correlated with ^{14}C dendrochronology, specific features in the atmospheric methane record, and outstanding climatic events (e.g., Younger Dryas, 12 800–11 650 yr ago; Termination II, 130 100 ± 2000 yr ago, etc.) identified by using stable isotope ratios and dust records may be adopted as tie points, depending on the core depth and the availability of information about the reference tie points.

In inland sites of Antarctica, however, the accumulation rates at some places are often less than ~ 30 mm water-equivalent yr^{-1}. Dome Fuji station (Fig. 1), located on a summit of Dronning Maud Land (DML) at an altitude of 3810 m a.s.l. (above sea level) (77°19′01″ S, 39°42′12″ E), is such an inland site in East Antarctica. The 10 m depth mean snow temperature at Dome Fuji is −57.3 °C (Kameda et al., 2008; Watanabe et al., 2003a), and the mean accumulation rate (MAR), measured from 1995 to 2006, was 27.3 ± 1.5 mm water-equivalent yr^{-1} (Kameda et al., 2008). The MARs at Dome Fuji derived for various time span are also given in Table 3a of Fujita et al. (2011), based on snow pit, firn core, and radar data studies.

The snow and ice at Dome Fuji have been recognized to contain much stratospheric information rather than tropospheric information. The direct evidence for this comes from tritium contents originated from the nuclear bomb tests in the 1960s; the tritium fallout at the Dome Fuji site is outstandingly high among 16 snow pit samples widely collected over Antarctica (Fourré et al., 2006).[1] Furthermore, chemical characteristics and ionic balance obtained at Dome Fuji are known to be completely different from those of sea-salt (Iizuka et al., 2006; Kamiyama et al., 1989; see also Bertler et al., 2005). These chemical properties support the fact that stratospheric constituents are most dominant in the precipitation environment at Dome Fuji than at those other 15 sites in Antarctica, in which South Pole, Dome C, Vostok, Talos Dome, and Halley Research Station are incorporated (see Fig. 2 of Fourré et al., 2006). The unique characteristic of the Dome Fuji site may be attributable to its high altitude (3810 m a.s.l.) and to its location substantially within the powerful polar vortex that develops in Antarctic winters.

Other drilling sites in Antarctica with low accumulation rates, besides Dome Fuji, include Dome C (25 mm water-equivalent yr^{-1}; EPICA community members, 2004),

---

[1] Note here that in Table 1 of Fourré et al. (2006), the highest value (4200 TU) was reported for Dome C. This, however, is wrong and the value is for Dome Fuji. In Kamiyama et al. (1989) that was quoted in Fourré et al. (2006) for the value concerned, the candidate Dome Fuji site was called as “DC” site, because the Dome Fuji station had not yet been constructed. The abbreviation “DC” in Kamiyama et al. (1987) was mistranslated into “Dome C” in Fourré et al. (2006).

Vostok (15–30 mm water-equivalent yr^{-1}; Ekaykin et al., 2004), Dome A (16 to 23 mm water-equivalent yr^{-1}; Xiao et al., 2008) and Plateau Remote (40 mm water-equivalent yr^{-1}; Cole-Dai et al., 2000). These sites are also shown in Fig. 1. In ice cores obtained at these sites, it is difficult to count annual layer signals. One of the reasons for this is postdepositional surface processes such as drifting. For example, missing layers associated with a negative or zero annual surface mass balance were estimated by the stake method to occur at a probability of 8.6 % at Dome Fuji (Kameda et al., 2008). Furthermore, a temporal resolution sufficient to detect seasonal variations is often difficult to obtain at low-accumulation sites. In deep cores drilled at such sites, the depth–age relationship is typically based on model calculations adjusted by using a number of chronological tie points (e.g., Parrenin et al., 2007a, b; Watanabe et. al., 2003b; Petit et al., 1999) or by correlation with variations in insolation or orbital tuning (e.g., Kawamura et al., 2007; Bender, 2002), or it is determined by transferring a more detailed age scale to the core in question (e.g., Ruth et al., 2007; Motoyama, 2007).

On the other hand, in shallow ice cores, modeling the densification process (Salamatin et al., 2009, and references therein) is a key issue in investigations of depth–density and hence depth–age relationships. Since such modeling is currently under development, chronologies of shallow cores drilled at low-accumulation sites are usually constructed by using known volcanic eruption dates as time horizon markers under the assumption that the accumulation rate between adjacent markers is constant (e.g., Igarashi et al., 2011; Ren et al., 2010; Cole-Dai et al., 2000; Watanabe et al., 1997). It is particularly difficult, however, to apply this method to date portions of shallow ice cores from before about AD 1260. From AD 1260 to the present, well-dated volcanic eruptions that can be correlated with volcanic sulfate spike signals in the core (see Sect. 2) are used as time horizon markers, whereas the dates of earlier volcanic eruptions are highly uncertain, resulting in a correspondingly large dating uncertainty in the core before AD 1260. Correlations between observed ^{10}Be variation in a core and ^{14}C records in tree rings has also been used to adjust absolute dates (e.g., Horiuchi et al., 2008).

The objective of this study was to construct a depth–age relationship in a Dome Fuji shallow ice core drilled in 2001 (hereafter DF01 core) as "correct" as possible for the last two millennia (except the last 100 yr; see Sect. 2). We used manually prepared samples with time resolutions of about 0.7 to 1 yr, a temporal resolution that is insufficient to count annual layer signals. To overcome the problems and uncertainties described above, we compared volcanic sulfate signals with those in a core (B32 core) in which annual layer counting was performed (Traufetter et al., 2004; Sommer et al., 2000a). The DML05 drilling site, where the B32 core was recovered, is about 1000 km apart from the Dome Fuji station (Fig. 1), and 1.7 km west (downstream direction) (Ruth et al., 2007) of Kohnen station, where the European Project for Ice Coring in Antarctica (EPICA) Dronning Maud Land (DML) deep core (EPICA community members, 2006) was later drilled. The chronology of the EPICA DML deep core is called EDML1 (Ruth et al., 2007).

In this study, we first synchronized the volcanic signals between the DF01 and B32 cores by comparing annually resolved non-sea-salt sulfate (nssSO_4^{2-}) concentrations between the two cores so that we could transfer the counted B32 chronology to the DF01 core. The transferred chronology is called the DFS1 (Dome Fuji Shallow ice core 1) chronology. Then, as Ruth and others (2007) correlated the B32 with the upper part of the EDML1 chronologies, we used this relation to transfer the top part of the EDML1 chronology, between AD 199 and 1170, to the DF01 chronology. This procedure created the DFS2 (Dome Fuji Shallow ice core 2) chronology. For the period before AD 199, only volcanic date information was available from the EDML1 chronology (M. Severi, personal communication, 2011). We thus assigned four volcanic eruption dates identified in the EPICA DML deep ice core between AD 1 and 199 to nssSO_4^{2-} spikes found in the DF01 core to make a tentative determination of the earliest part of the DFS2 chronology.

This paper is organized as follows. In Sect. 2, we describe the ice coring procedure and analyses of the DF01 core, and give a brief summary for the B32 and EDML1 time scales. In Sect. 3, we conduct volcanic signal matching between the B32 and

DF01 cores and present the DFS1 and DFS2 chronologies. Section 4 is devoted to the examination of possible errors in the DFS1 and DFS2 chronologies. We then compare in Sect. 5 the newly obtained chronologies with earlier efforts to construct a Dome Fuji shallow core age scale (Horiuchi et al., 2008; Watanabe et al., 1997) and consider their correspondence with volcanic eruption dates identified in WAIS Divide (Sigl et al., 2013), Law Dome (Plummer et al., 2012), and three Greenland ice cores (Dye-3, GRIP, NGRIP; Larsen et al., 2008). In Sect. 6, we present the MARs at Dome Fuji derived from the DFS1 and DFS2 chronologies. We finally summarize our conclusions in Sect. 7.

2 Properties of ice cores used in this study

In this section we describe the ice coring procedure and analyses of the DF01 core, and a brief summary for the B32 and EDML1 ages.

2.1 Ice coring and analyses of the DF01 core

At Dome Fuji, shallow firn cores were drilled in 1993, 1997, 1998, 2001, 2010, and 2011 by Japanese Antarctic Research Expedition (JARE) parties. In this work, we studied part of a 122 m long core drilled in 2001 (the DF01 core). In fact, the shallow DF01 core corresponds to the top part of the second Dome Fuji deep ice core, which used the same drilling hole. This deep core reached 3035.22 m; the ice at this depth has been preliminarily dated to 720 ka by synchronizing the δ^{18}O profile with that in ice core data from Dome C, for which a chronology has already been constructed (Motoyama, 2007; Dome Fuji ice core project members, in preparation). The DF01 firn core was cut into 50 cm long segments at Dome Fuji and transported to the National Institute of Polar Research (NIPR, Tokyo). Unfortunately, during the drilling, the top part of the DF01 core (1.8 to 7.7 m depth), which was composed of a very fragile depth hoar, was broken off and lost. We thus present here analyses of the part of the core below 7.7 m, that is, before about AD 1900 (see Sect. 3). As our purpose was to determine the detailed chronology of the DF01 core over the past 2000 yr, we analyzed the upper 85.5 m of the core.

In the sampling procedure, performed in the low-temperature room of NIPR, the 50 cm long segments of the DF01 core were further cut into 5 cm long (upper 20 m), 4 cm long (20–50 m), 3 cm long (50–75 m depth), and 2.5 cm long (> 75 m depth) samples. Depending on the depth, the temporal resolution of the samples usually ranged from about 0.7 to 1 yr, and was 0.9 yr on average. In each prepared sample, we measured ion concentrations (anions: SO_4^{2-}, Cl^-, NO_3^-, F^-, CH_3COO^-, $HCOO^-$, NO_2^-, $C_2O_4^{2-}$, PO_4^{3-}, $CH_3SO_4^-$; and cations: Na^+, K^+, Ca^{2+}, Mg^{2+}, NH_4^+). In this study, we used SO_4^{2-} and Cl^- concentrations measured by using a Dionex ICS2000 ion chromatography system at RIKEN (most measurements) and also a Dionex 500 system at NIPR (a very few of the very first measurements). In total, 2140 samples were analyzed in the present study. Ionic balance in the DF01 core will be discussed elsewhere.

2.2 A brief summary for B32 and EDML1 dates

The 150 m deep B32 core was obtained at point DML05 (Fig. 1) in the pre-site survey to determine the drilling place for the EPICA DML deep core. At both the DML05 and Kohnen sites, annual accumulation rates are sufficiently high, 60 kg m^{-2} yr^{-1} at the DML05 site (Sommer et al., 2000b) and 64 kg m^{-2} yr^{-1} at Kohnen station (Oerter et al., 2004). Annual layers in the B32 core have thus been counted by using seasonal variation in Na^+ concentrations to the bottom of the core, which corresponds to AD 165 ± 24 in the B32 chronology (Traufetter et al., 2004).

The ice coring, analyses, and dating determination procedure for the B32 core have been described in detail by Sommer et al. (2000a, b) and Traufetter et al. (2004). The oldest volcanic eruption identified by Traufetter et al. (2004) on the basis of their $nssSO_4^{2-}$ analyses dated to AD 186. The SO_4^{2-} and Cl^- concentrations in the B32 core used in this study were provided by H. Oerter and R. Weller (personal communication,

Title Page
Abstract | Introduction
Conclusions | References
Tables | Figures
◀| |▶
◀ ▶
Back | Close
Full Screen / Esc
Printer-friendly Version
Interactive Discussion

2011) and extended back to AD 172. The SO_4^{2-} concentrations in the B32 (DML05) core from AD 1998 back to AD 172 can also be found at the NOAA web site.[2]

Kohnen station is located on a very gentle slope (0.7 per mil; Ruth et al., 2007) where the horizontal flow velocity is 0.76 $m\,yr^{-1}$ (Wesche et al., 2007). Unlike dome sites such as Dome C and Dome Fuji, a realistic chronology cannot be determined for the EPICA DML deep core by using a 1-D glaciological ice flow model. Thus, the dating strategy used for the deep EPICA DML core was basically to transfer the Dome C (EDC3) chronology (Parrenin et al., 2007b), mainly through volcanic signal matching, thus creating the EDML1/EDC3 chronology (Ruth et al., 2007; Severi et al., 2007). Because the uppermost part of the EDC3 chronology is itself based on the B32 chronology, the upper 113 m of the EPICA DML deep ice core dates are based on the B32 chronology, and the part below 113 m was dated by transfer of the original EDC3 chronology. The B32 and EDML1/EDC3 chronologies are thus the same after AD 1170, the oldest volcanic eruption date from the B32 chronology adopted in the EDML1/EDC3 chronology. The EDML1/EDC3 time scale has been confirmed by a 3-D glaciological model (Huybrechts et al., 2007) that considered full ice flow dynamics and the upstream variations in the snow accumulation rate. The DFS2 chronology is thereby implicitly correlated with the EDC3 age as well, through the EDML1 age.

3 Volcanic signature synchronization and time scale results

Large volcanic eruptions send ash and gas into the air, and they can rise into the stratosphere. Sulfur dioxide and water vapor in the volcanic gases are subject to photochemical reactions, forming sulfate aerosol. The produced sulfate aerosol is transferred to polar regions by global atmospheric circulation and precipitates in Antarctica in 0–2 yr, depending on the latitude and the season of the eruption. This precipitation produces high concentration layer of sulfate that are observed as spikes in ice cores.

---

[2] http://www.ncdc.noaa.gov/paleo/metadata/noaa-icecore-6082.html

The non-sea-salt (nss)SO_4^{2-} concentration, which is used as the indicator of a volcanic eruption, is usually evaluated from the SO_4^{2-} and Na^+ concentrations as follows:

$$nssSO_4^{2-} = [SO_4^{2-}] - [SO_4^{2-}/Na^+]_{sw}[Na^+], \quad (1)$$

where $[SO_4^{2-}/Na^+]_{sw}$ is the ratio of SO_4^{2-} to Na^+ concentrations expressed as the standard mean chemical composition of seawater. In this work, however, Na^+ concentrations were not available from the B32 core so we used Cl^- concentrations instead. Thus,

$$nssSO_4^{2-} = [SO_4^{2-}] - [SO_4^{2-}/Cl^-]_{sw}[Cl^-] \quad (2)$$

Here, $[SO_4^{2-}/Cl^-]_{sw} = 0.140$ is the ratio of SO_4^{2-} to Cl^- mass concentrations in terms of the standard mean chemical composition of seawater. Using Cl^- concentration instead of Na^+ assumes that both the concentrations represent the sea-salt components at the same level. We confirmed that for the DF01 core, $nssSO_4^{2-}$ concentrations calculated using Eq. (2) are almost identical to those calculated with Eq. (1). It is also noted here that the sea-salt contribution, $[SO_4^{2-}/Cl^-]_{sw}$ $[Cl^-]$, obtained for Dome Fuji ice cores is very small: on average, sea-salt SO_4^{2-} contributed only 8 % of the total SO_4^{2-} concentration in this study (see also Iizuka et al., 2006, 2004; Hara et al., 2004).

Figure 2 shows a simplified overview of the synchronization of volcanic signals between the DF01 and B32 cores. Here, the volcanic $nssSO_4^{2-}$ fluxes obtained in the B32 core (Table 1 of Traufetter et al., 2004) are plotted against their water-equivalent depth (Fig. 2, lower panel), and DF01 $nssSO_4^{2-}$ concentrations are plotted against their water-equivalent depth simply multiplied by 2.34 (Fig. 2, upper panel). The synchronization of the volcanic signals between the two cores can be clearly seen in the figure with respect to both timing and $nssSO_4^{2-}$ amplitudes. Thus, given this simple, clear synchronization, the volcanic signal matching between the two cores is very unlikely to be misread. It is important to note here that the comparison is not against the true depth but against the water-equivalent depth, which makes the physical meaning clear. This simple matching in Fig. 2 implies that the MAR at Dome Fuji has been approximately 1/2.34 (∼ 0.43) of that at the B32 drilling site (DML05) over roughly the last 1800 yr (see below).

For detection of volcanic signals in sulfate ion concentrations with an approximately constant natural background, a variety of statistical methods have been applied in the preceding studies (Sigl et al., 2013; Moore et al., 2012; Gao et al., 2007; Kurbatov et al., 2006; Castellano et al., 2005, Traufetter et al., 2004). In particular, detailed sensitivity studies (Ferris et al., 2011; Gao et al., 2008) on the choice of the volcano detection procedure have shown that the results were robust for the different methods in detecting at least medium to large-scale volcanic events. To extract the volcanic signals from the DF01 nssSO_4^{2-} records in this study, we followed the same methodology adopted by Sigl et al. (2013). That is,

1. As a measure of the natural background, we applied a 31-point (approximately 0.9 yr × 30 = 27 yr) running median (RM) filter on the annually-resolved nssSO_4^{2-} time series.
2. The median of absolute deviation (MAD) provided a robust measure of variability in the data in the presence of “volcanic” peaks. Here an annual nssSO_4^{2-} value was assumed to be volcanic if it exceeds 3 × MAD above the RM.
3. The filter length of RM to approximate background variations and the detection threshold value of 3 × MAD were chosen empirically and validated using volcanic signals of well-known historic eruptions. Similar thresholds and filter length are used by Ferris et al. (2011) and Gao et al. (2006), as well as Sigl et al. (2013).

We thereby detected 94 “volcanic” peaks in the DF01 nssSO_4^{2-} time series (given in a Supplement table) by the above procedure. Combined with the detected volcanic peaks and the matching information from Fig. 2 consistently, we extend the single α value (= 2.34) used in Fig. 2 to multiple α values that are straightforwardly derived by accurate piecewise peak-to-peak matching. The α values obtained as well as the synchronized peak values of water-equivalent depths in the B32 and DF01 cores in each volcanic signal interval are listed in Table 1. It is clear in Table 1 that these α values fall within a very small range between 2.1 and 2.6, which supports our assertion that the overall synchronization is extremely good. Here each value of α means the inverse of the MAR at Dome Fuji relative to that at DML05 in the synchronized interval in question.

The detailed peak-to-peak nssSO_4^{2-} synchronization between the two cores is shown in Fig. 3, where on the bottom horizontal axes not only the water-equivalent depth of the B32 core is shown, as in Fig. 2, but also the water-equivalent depth of the DF01 core multiplied by α in each synchronized interval. With this synchronization the B32 chronology was transferred to the DFS1 (Dome Fuji shallow ice core (1) chronology under the assumption that the DF01 accumulation rate between synchronized volcanic time horizons was constant. The DFS1 chronology is shown above the top horizontal axes in Fig. 3. As mentioned in Sect. 1, Ruth et al. (2007) published the relationship between the B32 and EDML1/EDC3 chronologies. We used this relation to transfer the EDML1/EDC3 chronology to the DFS2 (Dome Fuji shallow ice core (2) chronology, again under the assumption that the DF01 accumulation rate between the synchronized horizons was constant. As the EDML1/EDC3 chronology is the same as the B32 chronology for the period after AD 1170 (see Ruth et al., 2007), we show the DFS2 chronology only before AD 1170 in Fig. 3 (below the top horizontal axes). Note that the oldest eruption identified in the B32 shallow core occurred in AD 187, which corresponds to AD 199 in the EDML1 chronology (Ruth et al., 2007); the corresponding eruption is shown in Fig. 3 at the right-hand edge of the lower panel. In Fig. 3 one should compare the difference in the scale of the ordinate between the upper and lower panels, and then can easily recognize that volcanic activity was high in the last millennium but before that period the volcanic activity was much weaker, having resulted in the difficulty in constructing a shallow ice core chronology based on volcanic eruption signals.

We also have information on four additional volcanic eruption dates between AD 199 and AD 1 in the EDML1/EDC3 chronology, obtained from the upper part of the EPICA deep ice core (M. Severi, personal communication, 2011); these eruptions occurred in AD 172, 153, 19, and 8 (Table 2). We used these dates to identify the corresponding volcanic signals in the DF01 nssSO_4^{2-} concentrations. It is confirmed that the MARs based on this tentative volcanic matching for the period from AD 199 back to AD 8 are reasonable when compared with other MARs (see Table 3). We then assumed the same MAR (26.5 mm yr^{-1}) from AD 8 to AD 1 as that between AD 19 and 8 in order to extend the DFS2 chronology back to AD 1.

The resulting depth–age relationship in the DFS1 and DFS2 chronologies is shown in Fig. 4a, and their difference is depicted in Fig. 4b. One sees in Fig. 4b that the absolute DFS1 age is systematically older than the corresponding DFS2 age before AD 1170. It is mentioned here that radar measurements of the ice sheet between Dome Fuji and Kohnen station have been performed recently (Steinhage et al., 2013; Fujita et al., 2011). Of these, Steinhage and colleagues (2013) reported radar isochrone horizons between the two sites for deep depths; the shallowest isochronous layer has been given between 338 m depth at Konen and 166 m depth at Dome Fuji. Deeper than depths concerned in this study (< 85 m depth for DF01), this could not be used for checking the consistency with the volcanic synchronization between the two sites.

4 Uncertainty in DFS1 and DFS2 chronologies

In this section we evaluate the uncertainty in the obtained DFS1 and DFS2 chronologies, which consists of absolute dating uncertainty and the interpolation uncertainty. In the following we treat these one by one.

4.1 Absolute dating uncertainty

The absolute errors in the stratigraphic time horizons in the DFS1 chronology depend directly on those in the B32 chronology. The B32 errors have been reported by Traufetter et al. (2004), and are also listed in Table 1. The error range is relatively small (±1–5 yr) after around AD 1260, and then it increases linearly to ±23 yr in AD 187, the oldest eruption identified (Traufetter et al., 2004). On the other hand, the errors in the volcanic horizons in the DFS2 chronology depend on those in the EDC3 chronology (Parrenin et al., 2007b), because the EDML1 age (Ruth et al., 2007) is based on EDC3. The match point of the EDC3 chronology before AD 1170 comes from a specific feature of the ^{10}Be concentrations in the Dome C (EDC96) core, which was correlated with a similar feature in the ^{14}C concentration profile in tree rings observed at 765 BC, for which an error of ±50 yr has been estimated (Parrenin et al., 2007b). Therefore, by changing the date of the match point from 765 BC to 715 (= 765 – 50) BC or to 815 (= 765 + 50) BC, we can easily estimate the absolute dating error in the EDML1/EDC3 chronology. These estimated errors are shown in Table 2. Coincidentally, the errors in the B32 and EDC3 chronologies are comparable in the time range from AD 1170 back to around AD 200.

Very recently it was insisted that the timing of the Kuwae eruption occurring in ice cores is not around AD 1453 as previously thought, but around AD 1458, based on precise annual layer dating (Sigl et al., 2013; Plummer et al., 2012). Our matching reference here, Traufetter and others (2004), derived AD 1453±5 as the year of deposition of the Kuwae eruption. This is marginally consistent with the newly proposed eruption date within the error; we thus follow the original work of Traufetter et al. (2004), and do not shift the tie-point date in this study. We also note that the last Taupo eruption was recently assigned a new date (AD 230 ± 16 ; Siebert et al., 2010; Sparks, 2004). The Taupo eruption date (AD 187) identified in Traufetter et al. (2004) may thus be replaced by this newly assigned date. Careful inspection of Table 1 of Traufetter et al. (2004) shows that another eruption candidate peak at AD 221 ± 22 just after the AD 187 eruption in their study may be instead attributable to the last “AD 230” Taupo eruption, which was shown in Table 1.

4.2 Interpolation uncertainty between the stratigraphic match points

The DFS1 and DFS2 chronologies were both constructed under the assumption that the accumulation rates between the synchronized volcanic time horizons were constant. The dating uncertainty arising from this assumption should therefore be taken into account in addition to the absolute dating error of each time horizon.

Ruth et al. (2007) investigated possible interpolation errors in the EDML1 chronology, for which a piecewise cubic Herimite method was applied to interpolate between the match points. By a discerning statistical analysis they reported that the expected maximal interpolation error, $E_{\mathrm{rr}}^{\max}$, can be as large as ±15 % of the age gap to the nearest match point, t_{nearest}, as expressed through $E_{\mathrm{rr}}^{\max} = (15 \pm 6\,\mathrm{yr})/100\,\mathrm{yr} \times t_{\mathrm{nearest}}$ (Ruth et al., 2007). By performing a similar analysis of the DFS1 and DFS2 ages, we found expected maximal interpolation errors of the same magnitude (±15 %).

5 Comparison with preceding studies

Here we confine ourselves to a discussion of the differences of DFS1 and DFS2 ages compared with earlier work on Dome Fuji shallow ice core dates for before AD 1260, because the main accomplishment of this study was the establishment of a chronology for before that date.

Watanabe et al. (1997) conducted a preliminary dating study of the Dome Fuji 1993 (DF93) shallow ice core in which they identified five major peaks in the ECM profile at depths of 29.1, 37.8, 60.4, 69.2, and 97.8 m and correlated them with five known volcanic eruptions that occurred in AD 1464, 1259, 865, 639, and 346 BC, respectively. Taking into account that depths in the DF01 core are 1 m deeper than depths in the DF93 core, we found a clear nssSO_4^{2-} spike in the DF01 core at the position corresponding to the ECM peak at 69.2 m depth in the DF93 core. In our chronologies, however, this peak was not dated to AD 639; it corresponded to AD 442 ± 17 in the DFS1/B32 time scale and to AD 460 ± 19 in the DFS2/EDML1/EDC3 time scale. Although an AD 636 ± 15 eruption peak was identified in the B32 core (Traufetter et al., 2004), no peak at that date was identified in the EPICA DML deep core (Ruth et al., 2007) and in the DF01 core of the present study. The AD 865 eruption peak used as a time marker by Watanabe et al. (1997) was not identified in the B32 core, and hence there is no correspondence to this peak in the DF01 core. The preliminary chronology proposed by Watanabe et al. (1997) is compared with the DFS1 and DFS2 ages in Fig. 5. A large difference of Watanabe et al. (1997) from DFS1 and DFS2 ages found in Fig. 5 can be attributed to the use of known volcanic dates alone without any guide, when stratigraphic volcanic records are rather uncertain and volcanic signals are much weaker than those of the last millennium.

For the DF01 core, Horiuchi et al. (2008) proposed a chronology for the period between AD 1900 and 700 based on ^{10}Be-^{14}C profile matching. This chronology is also shown in Fig. 5 from AD 1815 back to 755 using the values given in Table 2 of Horiuchi et al. (2008). We found from Fig. 5 that the ^{10}Be-^{14}C dating proposed by Horiuchi et al. (2008) is very close to the DFS1 and DFS2 chronologies between about AD 1100 and 800, where dating by using only known volcanic dates is difficult, as mentioned above.

We now consider correspondence of the DFS1 and DFS2 ages with volcanic eruption dates before AD 1170 reported in preceding studies, attempting to see whether the DFS1 or the DFS2 chronology is more consistent. Selected large volcanic eruption dates before AD 1170 identified from WAIS Divide (Sigl et al., 2013) and from Law Dome (Plummer et al., 2012), both from Antarctica (Fig. 1), are listed in Table 4. In addition, three volcanic eruption dates before AD 1170 (adopted from Larsen et al., 2008) identified in three (Dye-3, GRIP, NGRIP) Greenland ice cores sharing the GICC05 chronology (Vinther et al., 2006) are listed in Table 4. Not all volcanic signals observed in Greenland will necessarily also be observable in Antarctica, but those three eruptions observed in Greenland were regarded by Larsen et al. (2008) as large eruptions that affected both hemispheres. In particular, the "AD 536" event has been suggested to have been a very large eruption, even surpassing the Tambora eruption in AD 1815. We also show in Table 4 the candidate corresponding signals for these eruptions in the DFS1 and DFS2 chronologies. One may see in Table 4 that the DFS2 chronology, at least in early (before about AD 330) ages, appears to be more accordant with the observed eruption dates previously identified at the WAIS Divide and Law Dome. Overall, however, it is difficult to conclude whether the DFS1 or the DFS2 time scale is more consistent with the preceding studies, because of the absolute error of the time scales.

6 Mean accumulation rate at Dome Fuji

Table 3 lists the absolute mean accumulation rates (MARs) at Dome Fuji based on the DFS1 age, the MARs at Dome Fuji relative to those at DML05 (i.e., the inverse of α in Table 1), and the MARs at Dome Fuji based on the DFS2 age. It is shown in Table 3 that the MAR after the Tambora eruption (AD 1815) was clearly increased. After other large eruptions (AD 1454, Kuwae, and AD 1258, Samalas), however, such a tendency of a MAR enhancement cannot be found for the synchronized interval in this work.

We depict in the upper panel of Fig. 6 the MARs derived at Dome Fuji against the DFS1 ages (red lines; bottom axis) and against the DFS2 ages (blue line; top axis). The MARs derived from the four tentatively identified eruptions between AD 199 and 1 in the DFS2 chronology are shown by the dashed line. The MARs show a variation of ±20 % in both the DFS1 and DFS2 chronologies for the period from AD 1900 back to 200. For comparison, annual accumulation rates are known to vary by ±30 % at DML05, the B32 drilling site (Sommer et al., 2000b). In the lower panel of Fig. 6, the relative MAR (Table 3) is plotted against the DFS1 age in order to show the MARs at Dome Fuji relative to those at DML05. These relative MARs do not vary substantially but remain between 0.38 to 0.48 from AD 1900 back to 200, again showing extremely good synchronization.

It is worth mentioning here that the MAR values become less variable as the size of the synchronized interval increases. This occurs because higher variations are averaged out in larger domains. We can observe this feature, for example, in the MAR between AD 1170 and 686 in the DFS1 chronology and in that between AD 1170 and 699 corresponding in the DFS2 chronology. The volcanic time markers constructing this particular interval is separated by nearly 500 yr. It is very difficult to imagine that the MAR was nearly constant over such a long period, and the MAR values will therefore likely show more variation when additional time markers are introduced in the domain. Note that MAR values are always meaningful in a set within the averaged interval, whereas a single value at a local point is not.

7 Conclusions

In this study, we synchronized nssSO_4^{2-} concentrations between the DF01 and B32 shallow cores to derive a DFS1 chronology from AD 1900 down to 187. EDML1 ages correlated with B32 volcanic signals were used to derive a DFS2 chronology, which extends back to AD 199, and this was tentatively extended further back to AD 1 by using additional volcanic eruption dates (M. Severi, personal communication, 2011). In particular, the period before around AD 1260 is here dated with relatively high resolution for the first time in a Dome Fuji shallow core.

The DFS1 and DFS2 chronologies described in this study at present provide the most detailed available depth–age relation for Dome Fuji shallow ice cores. The chronology data are given in a Supplement table along with the time series data of the SO_4^{2-}, Cl^-, and nssSO_4^{2-} concentrations. These time scales will have many useful applications to, for example, volcanic flux calculations and climate changes in the past, with using the DF01 core as well as fresher cores drilled in 2010 and 2011 around Dome Fuji, a very unique precipitation site in an inland site of Antarctica.

Supplementary material related to this article is available online at http://www.the-cryosphere-discuss.net/8/769/2014/tcd-8-769-2014-supplement.pdf.

Acknowledgements. We are very grateful to H. Oerter and R. Weller for providing us with the B32 core data and for their encouraging discussion. We also acknowledge M. Severi for providing us with the EDML1 dates for volcanic eruptions before AD 199. We thank Y. Fujii and Y. Iizuka for their helpful discussions, and all members of the Dome Fuji drilling team and the JARE-42 party, as well as those who participated in sampling the DF01 core at NIPR between 2004 and 2009. We are indebted to T. Kobayashi and M. Kitagawa for their help to get some of the ionic concentrations used in this study. This work was supported in part by Funding Program for Next Generation World-Leading Researchers (NEXT Program, Grant Number GR098) initiated by the Council for Science and Technology Policy and Japan Society for the Promotion of Science (JSPS) and a Grant-in-Aid for Scientific Research (A) (Grant Number 22244015) from JSPS.

References

Bender, M. L.: Orbital tuning chronology for the Vostok climate record supported by trapped gas composition, Earth Planet. Sc. Lett., 204, 275–289, 2002.

Bertler, N., Mayewski, P. A., Aristarain, A., Barrett, P., Becagli, S., Bernardo, R., Bo, S., Xiao, C., Curran, M., Qin, D., Dixon, D., Ferron, F., Fischer, H., Frey, M., Frezzotti, M., Fundel, F., Genthon, C., Gragnani, R., Hamilton, G., Handley, M., Hong, S., Isaksson, E., Kang, J., Ren, J., Kamiyama, K., Kanamori, S., Kärkäs, E., Karlöf, L., Kaspari, S., Kreutz, K., Kuravatov, A., Meyerson, E., Ming, Y., Zhang, M., Motoyama, H., Mulvaney, R., Oerter, H., Osterberg, E., Proposito, M., Pyne, A., Ruth, U., Simões, J., Smith, B., Sneed, S., Teinilä, K., Traufetter, F., Udiski, R., Virkkula, A., Watanabe, O., Williamson, B., Winther, J.-G., Li, Y., Wolff, E., Li, Z., Zielinski, A.: Snow chemistry across Antarctica, Ann. Glaciol., 41, 167–179, 2005.

Budner, D., and Cole-Dai, J.: The number and magnitude of large explosive volcanic eruptions between 904 and 1865 AD: quantitative evidence from a new South Pole ice core, in: Volcanism and the Earth's Atmosphere, Geoph. Monog. Series, 139, 165–176, 2003.

Castellano, E., Becagli, S., Hansson, M., Hutterli, M., Petit, J. R., Rampino, M. R., Severi, M., Steffensen, J. P., Traversi, R., and Udisti, R.: Holocene volcanic history as recorded in the sulfate stratigraphy of the European project for ice coring in AntarcticaDome C (EDC96) ice core, J. Geophys. Res., 110, D06114, doi:10.1029/2004JD005259, 2005.

Cole-Dai, J., Mosley-Thompson, E., Wight, S. P., and Thompson, L. G.: A 4100 yr record of explosive volcanism from an East Antarctica ice core, J. Geophys. Res., 105, 24431–24441, 2000.

Ekaykin, A. A., Lipenkov, V. Ya., Kuzmina, I. N., Petit, J. R., Masson-Delmotte, V., and Johnsen, S. J.: The changes in isotope composition and accumulation of snow at Vostok station, East Antarctica, over the past 200 yr, Ann. Glaciol., 39, 569–575, 2004.

EPICA community members: Eight glacial cycles from an Antarctic ice core, Nature, 429, 623–628, doi:10.1038/nature02599, 2004.

EPICA community members: One-to-one coupling of glacial climate variability in Greenland and Antarctica, Nature, 444, 195–198, doi:10.1038/nature05301, 2006.

Ferris, D. G., Cole-Dai, J., Reyes, A. R., and Budner, D. M.: South Pole ice core record of explosive volcanic eruptions in the first and second millennia AD, and evidence of a large eruption in the tropics around 535 AD, J. Geophys. Res., 116, D17308, doi:10.1029/2011JD015916, 2011.

Fourré, E., Jean-Baptiste, P., Dapoigny, A., Baumier, D., Petit, J.-R., and Jouzel, J.: Past and recent tritium levels in Arctic and Antarctic polar caps, Earth Planet. Sc. Lett., 245, 56–64, 2006.

Fujii, Y., Kamiyama, K., Shoji, H., Narita, H., Nishio, F., Kameda, T., and Watanabe, O.: 210 yr ice core records of dust storms, volcanic eruptions and acidification at Site-J, Greenland, Mem. Natl. Inst. Polar Res., 54, 209–220, 2001.

Fujita, S., Holmlund, P., Andersson, I., Brown, I., Enomoto, H., Fujii, Y., Fujita, K., Fukui, K., Furukawa, T., Hansson, M., Hara, K., Hoshina, Y., Igarashi, M., Iizuka, Y., Imura, S., Ingvander, S., Karlin, T., Motoyama, H., Nakazawa, F., Oerter, H., Sjöberg, L. E., Sugiyama, S., Surdyk, S., Ström, J., Uemura, R., and Wilhelms, F.: Spatial and temporal variability of snow accumulation rate on the East Antarctic ice divide between Dome Fuji and EPICA DML, The Cryosphere, 5, 1057–1081, doi:10.5194/tc-5-1057-2011, 2011.

Gao, C., Robock, A., Self, S., Witter, J. B., Steffenson, J. P., Clausen, H. B., Siggaard-Andersen, M. L., Johnsen, S., Mayewski, P. A., and Ammann, C.: The 1452 or 1453 AD

Kuwae eruption signal derived from multiple ice core records: greatest volcanic sulfate event of the past 700 years, J. Geophys. Res., 111, D12107, doi:10.1029/2005JD006710, 2006.

Gao, C., Oman, L., Robock, A., and Stenchikov, G. L.: Atmospheric volcanic loading derived from bipolar ice cores: accounting for the spatial distribution of volcanic deposition, J. Geophys. Res., 112, D09109, doi:10.1029/2006JD007461, 2007.

Gao, C., Robock, A., and Ammann, C.: Volcanic forcing of climate over the past 1500 yr: an improved ice core-based index for climate models, J. Geophys. Res., 113, D23111, doi:10.1029/2008JD010239, 2008.

Hara, K., Osada, K., Kido, M., Hayashi, M., Matsunaga, K., Iwasaka, Y., Yamanouchi, T., Hashida, G., and Fukatsu, T.: Chemistry of sea-salt particles and inorganic halogen species in Antarctic regions: compositional differences between coastal and inland stations, J. Geophys. Res., 109, D20208, doi:10.1029/2004JD004713, 2004.

Horiuchi, K., Uchida, T., Sakamoto, Y., Ohta, A., Matsuzaki, H., Shibata, Y., and Motoyama, H.: Ice core record of ^{10}Be over the past millennium form Dome Fuji, Antarctica: a new proxy record of past solar activity and a powerful tool for stratigraphic dating, Quat. Geochronol., 3, 253–261, 2008.

Huybrechts, P., Rybak, O., Pattyn, F., Ruth, U., and Steinhage, D.: Ice thinning, upstream advection, and non-climatic biases for the upper 89 % of the EDML ice core from a nested model of the Antarctic ice sheet, Clim. Past, 3, 577–589, doi:10.5194/cp-3-577-2007, 2007.

Igarashi, M., Nakai, Y., Motizuki, Y., Takahashi, K., Motoyama, H., and Makishima, K.: Dating of the Dome Fuji shallow ice core based on a record of volcanic eruptions from AD 1260 to AD 2001, Polar Sci., 5, 411–420, 2011.

Iizuka, Y., Fujii, Y., Hirasawa, N., Suzuki, T., Motoyama, H., Furukawa, T., and Hondoh, T.: SO_4^{2-} minimum in summer snow layer at Dome Fuji, Antarctica, and the probable mechanism, J. Geophys. Res., 109, D04307, doi:10.1029/2003JD004138, 2004.

Iizuka, Y., Hondoh, T., and Fujii, Y.: Na_2SO_4 and $MgSO_4$ salts during the Holocene period derived by high-resolution depth analysis of a Dome Fuji ice core, J. Glaciol., 52, 58–64, 2006.

Kameda, T., Motoyama, H., Fujita, S., and Takahashi, S.: Temporal and spatial variability of surface mass balance at Dome Fuji, East Antarctica, by the stake method from 1995 to 2006, J. Glaciol., 54, 107–116, 2008.

Kamiyama, K., Ageta, Y., and Fujii, Y.: Atmospheric and depositional environments traced from unique chemical compositions of the snow over an inland high plateau, Antarctica, J. Geophys. Res., 94, 18515–18519, 1989.

Kawamura, K., Parrenin, F., Lisiecki, L., Uemura, R., Vimeux, F., Severinghaus, J. P., Hutterli, M. A., Nakazawa, T., Aoki, S., Jouzel, J., Raymo, M. E., Matsumoto, K., Nakata, H., Motoyama, H., Fujita, S., Goto-Azuma, K., Fujii, Y., and Watanabe, O.: Northern Hemisphere forcing of climatic cycles in Antarctica over the past 360,000 yr, Nature, 448, 912–916, 2007.

Kohno, M. and Fujii, Y.: Past 220 yr bipolar volcanic signals: remarks on common features of their source volcanic eruptions, Ann. Glaciol., 35, 217–223, 2002.

Kurbatov, A. V., Zielinski, G. A., Dunbar, N. W., Mayewski, P. A., Meyerson, E. A., Sneed, S. B., and Taylor, K. C.: A 12,000 yr record of explosive volcanism in the Siple Dome Ice Core, West Antarctica, J. Geophys. Res., 111, D12307, doi:10.1029/2005JD006072, 2006.

Larsen, L. B., Vinther, B. M., Briffa, K. R., Melvin, T. M., Clausen, H. B., Jones, P. D., Siggaard-Andersen, M.-L., Hammer, C. U., Eronen, M., Grudd, H., Gunnarson, B. E., Hantemirov, R. M., Naurzbaev, M. M., and Nicolussi, K.: New ice core evidence for a volcanic cause of the AD 536 dust veil, Geophys. Res. Lett., 35, L04708, doi:10.1029/2007GL032450, 2008.

Lavigne, F., Degeai, J.-P., Komorowski, J.-C., Guillet, S., Robert, V., Lahitte, P., Oppenheimer, C., Stoffel, M., Vidal, C. M., Surono, Pratomo, I., Wassmer, P., Hajdas, I., Hadmoko, D. S., and de Belizal, E.: Source of the great AD 1257 mystery eruption unveiled, Samalas volcano, Rinjani Volcanic Complex, Indonesia, P. Natl. Acad. Sci. USA, 110, 16742–16747, doi:10.1073/pnas.1307520110, 2013.

Moore, J. C., Beaudon, E., Kang, S., Divine, D., Isaksson, E., Pohjola, V. A., and van de Wal, R. S. W.: Statistical extraction of volcanic sulphate from non polar ice cores, J. Geophpys. Res., 117, D03306, doi:10.1029/2011JD016592, 2012.

Motoyama, H.: The second deep ice coring project at Dome Fuji, Antarctica, Sci. Drill., 5, 41–43, doi:10.2204/iodp.sd.5.05.2007, 2007.

Oerter, H., Graf, W., Meyer, H., and Wilhelms, F.: The EPICA ice core from Dronning Maud Land: first results from stable-isotope measurements, Ann. Glaciol., 39, 307–312, 2004.

Palmer, A. S., van Ommen, T. D., Curran, M. A. J., Morgan, V., Souney, J. M., Mayewski, P. A.: High-precision dating of volcanic events (AD 1301–1995) using ice cores from Law Dome, Antarctica, J. Geophpys. Res., 106, 28089–28095, 2001.

Parrenin, F., Dreyfus, G., Durand, G., Fujita, S., Gagliardini, O., Gillet, F., Jouzel, J., Kawamura, K., Lhomme, N., Masson-Delmotte, V., Ritz, C., Schwander, J., Shoji, H., Uemura, R., Watanabe, O., and Yoshida, N.: 1-D-ice flow modelling at EPICA Dome C and Dome Fuji, East Antarctica, Clim. Past, 3, 243–259, doi:10.5194/cp-3-243-2007, 2007a.

Parrenin, F., Barnola, J.-M., Beer, J., Blunier, T., Castellano, E., Chappellaz, J., Dreyfus, G., Fischer, H., Fujita, S., Jouzel, J., Kawamura, K., Lemieux-Dudon, B., Loulergue, L., Masson-Delmotte, V., Narcisi, B., Petit, J.-R., Raisbeck, G., Raynaud, D., Ruth, U., Schwander, J., Severi, M., Spahni, R., Steffensen, J. P., Svensson, A., Udisti, R., Waelbroeck, C., and Wolff, E.: The EDC3 chronology for the EPICA Dome C ice core, Clim. Past, 3, 485–497, doi:10.5194/cp-3-485-2007, 2007b.

Petit, J. R., Jouzel, J., Raynaud, D., Barkov, N. I., Barnola, J.-M., Basile, I., Bender, M., Chappellaz, J., Davis, M., Delaygue, G., Delmotte, M., Kotlyakov, V. M., Legrand, M., Lipenkov, V. Y., Lorius, C., Pépin, L., Ritz, C., Saltzman, E., and Stievenard, M.: Climate and atmospheric history of the past 420,000 yr from the Vostok ice core, Antarctica, Nature, 399, 429–436, 1999.

Plummer, C. T., Curran, M. A. J., van Ommen, T D., Rasmussen, S. O., Moy, A. D., Vance, T. R., Clausen, H. B., Vinther, B. M., and Mayewski, P. A.: An independently dated 2000-yr volcanic record from Law Dome, East Antarctica, including a new perspective on the dating of the 1450s CE eruption of Kuwae, Vanuatu, Clim. Past, 8, 1929–1940, doi:10.5194/cp-8-1929-2012, 2012.

Ren, J., Li, C., Hou, S., Xiao, C., Qin, D., Li, Y., and Ding, M.: A 2680 yr volcanic record from the DT-401 East Antarctic ice core, J. Geophys. Res., 115, D11301, doi:10.1029/2009JD012892, 2010.

Ruth, U., Barnola, J.-M., Beer, J., Bigler, M., Blunier, T., Castellano, E., Fischer, H., Fundel, F., Huybrechts, P., Kaufmann, P., Kipfstuhl, S., Lambrecht, A., Morganti, A., Oerter, H., Parrenin, F., Rybak, O., Severi, M., Udisti, R., Wilhelms, F., and Wolff, E.: “EDML1”: a chronology for the EPICA deep ice core from Dronning Maud Land, Antarctica, over the last 150 000 years, Clim. Past, 3, 475–484, doi:10.5194/cp-3-475-2007, 2007.

Salamatin, A. N., Lipenkov, V. Ya., Barnola, J. M., Hori, A., Duval, P., and Hondoh, T.: Snow/firn densification in polar ice sheets, in: Low Temperature Science Suppl. Issue, 68, Physics of Ice Core Record II, edited by: Hondoh, T., Nire Printing, Sapporo, Japan, 195–222, 2009.

Severi, M., Becagli, S., Castellano, E., Morganti, A., Traversi, R., Udisti, R., Ruth, U., Fischer, H., Huybrechts, P., Wolff, E., Parrenin, F., Kaufmann, P., Lambert, F., and Steffensen, J. P.: Synchronisation of the EDML and EDC ice cores for the last 52 kyr by volcanic signature matching, Clim. Past, 3, 367–374, doi:10.5194/cp-3-367-2007, 2007.

Siebert, L., Simkin, T., and Kimberly, P.: Volcanoes of the World, 3rd edn., University of California Press, Berkeley, 551 pp., 2010.

Sommer, S., Wagenbach, D., Mulvaney, R., and Fischer, H.: Glacio-chemical study spanning the past 2 kyr on three ice cores from Dronnning Maud Land, Antarctica 2. Seasonally resolved chemical records, J. Geophys. Res., 105, 29423–29433, 2000a.

Sommer, S., Appenzeller, C., Röthlisberger, R., Hutterli, M. A., Stauffer, B., Wagenbach, D., Oerter, H., Wilhelms, F., Miller, H., Mulvaney, R.: Glacio-chemical study spanning the past 2kyr on three ice cores from Dronnning Maud Land, Antarctica 1. Annually resolved accumulation rates, J. Geophys. Res., 105, 29411–29421, 2000b.

Sigl, M., McConnell, J. R., Layman, L., Maselli, O., McGwire, K., Pasteris, D., Dahl-Jensen, D., Steffensen, J. P., Vinther, B., Edwards, R., Mulvaney, R., Kipfstuhl, S.: A new bipolar ice core record of volcanism from WAIS Divide and NEEM and implications for climate forcing of the last 2000 yr, J. Geophys. Res.-Atmos., 118, 1–19, doi:10.1029/2012JD018603, 2013.

Sparks, R.: Radiocarbon dating – New Zealand beginnings, New Zealand Science Review, 61, 39–41, 2004.

Steinhage, D., Kipfstuhl, S., Nixdorf, U., and Miller, H.: Internal structure of the ice sheet between Kohnen station and Dome Fuji, Antarctica, revealed by airborne radio-echo sounding, Ann. Glaciol., 54, 163–167, doi:10.3189/2013AoG64A113, 2013.

Taylor, K. C., Alley, R. B., Meese, D. A., Spencer, M. K., Brook, E. J., Dunbar, N. W., Finkel, R. C., Gow, A. J., Kurbatov, A. V., Lamorey, G. W., Mayewski, P. A., Meyerson, E. A., Nishiizumi, K., and Zielinski, G. A.: Dating the Siple Dome (Antarctica) ice core by manual and computer interpretation of annual layering, J. Glaciol., 50, 453–461, 2004.

Traufetter, F., Oerter, H., Fischer, H., Weller, R., and Miller, H.: Spatio-temporal variability in volcanic sulphate depotision over the past 2 kyr in snow pits and firn cores from Amundsenisen, Antarctica, J. Glaciol., 50, 137–146, 2004.

Vinther, B. M., Clausen, H. B., Johnsen, S. J., Rasmussen, S. O., Andersen, K. K., Buchardt, S. L., Dahl-Jensen, D., Seierstad, I. K., Siggaard-Andersen, M.-L., Steffensen, J. P., Svensson, A., Olsen, J., and Heinemeier, J.: A synchronized dating of three Greenland ice cores throughout the Holocene, J. Geophys. Res., 111, D13102, doi:10.1029/2005JD006921, 2006.

Watanabe, O., Fujii, Y., Motoyama, H., Furukawa, T., Shoji, H., Enomoto, H., Kameda, T., Narita, H., Naruse, R., Hondoh, T., Fujita, S., Mae, S., Azuma, N., Kobayashi, S., Nakawo, M., and Ageta, Y.: A preliminary study of ice core chronology at Dome Fuji station, Antarctica, Proc. NIPR Symp. Polar Meteorol. Glaciol., 11, 9–13, 1997.

Watanabe, O., Kamiyama, K., Motoyama, H., Fujii, Y., Igarashi, M., Furukawa, T., Goto-Azuma, K., Saito, T., Kanamori, S., Kanamori, N., Yoshida, N., and Uemura, R.: General tendencies of stable isotopes and major chemical comstituents of the Dome Fuji deep ice core, Mem. Natl. Inst. Polar Res., Spec. Issue, 57, 1–24, 2003a.

Watanabe, O., Shoji, H., Satow, K., Motoyama, H., Fujii, Y., Narita, H., and Aoki, S.: Dating of the Dome Fuji, Antarctica deep ice core, Mem. Natl. Inst. Polar Res., Spec. Issue, 57, 25–37, 2003b.

Wesche, C., Eisen, O., Oerter, H., Schulte, D., and Steinhage, D.: Surface topography and ice flow in the vicinity of EDML deep-drilling site, J. Glaciol., 53, 442–448, 2007.

Xiao, C., Li, Y., Hou, S., Allison, I., Bian, L., Ren, J.: Preliminary evidence indicating Dome A (Antarctica) satisfying preconditions for drilling the oldest ice core, Chinese Sci. Bull., 53, 102–106, 2008.

Table 1. The B32 volcanic eruption chronology and its synchronization with the DF01 core, AD 1900–187.

No.	Year of Eruption (AD)	Volcanic Eruption Possibly Associated with Detected Event	VEI	B32 Depth[a] (m.w.e.)	B32 Age[a] (AD)	Synchronization, this work	DF01 Depth (m.w.e.)	α[b]
1	1889	difficult to be identified in B32 data[c]						
2	1886	difficult to be identified in B32 data[c]						
3	1883	Krakatau, Indonesia	6	7.24	1883.5 ± 1	∗	3.40	2.54
4	1835	Cosiguina, Nicaragua	5	10.21	1834.5 ± 1	∗	4.57	2.28
5	1815	Tambora, Indonesia	7	11.39	1816.5 ± 1	∗	5.09	2.58
6	1809±2	unknown		11.80	1809.5 ± 3	∗	5.24	2.35
7	1762	Planchon-Peteroa, Chile	4	14.77	1762.0 ± 1			
8	1693[d]	Serua, Indonesia?[d]	4?	18.71	1695.5 ± 3	∗	8.18	2.50
9	1691	Reventador, Ecuador?	3	19.08	1691.0 ± 3			
10	1673	Gamkonora, Indonesia	5?	19.93	1675.5 ± 3	∗	8.67	2.48
11	1641	Parker, Philippines	5?	21.85	1639.5 ± 1	∗	9.44	2.10
12		unknown[d]		23.05	1619.5 ± 1	∗	10.01	2.39
13	1600	Huaynaputina, Peru	6	24.24	1601.5 ± 1	∗	10.51	2.20
14	1595	Ruiz, Colombia	4	24.61	1595.5 ± 3	∗	10.68	2.48
15	1541[d]	Reentador, Ecuador?[d]	3	27.84	1542.0 ± 5			
16	1452±10[e]	Kuwae, SW Pacific	6	32.93	1454.5 ± 5	∗	14.03	2.34
17		unknown		37.62	1375.5 ± 5			
18	1330 ± 75[d]	Cerro Bravo, Colombia	4	39.76	1342.5 ± 5	∗	16.95	2.28
19		unknown		43.27	1284.5 ± 5	∗	18.49	2.24
20		unknown		43.76	1276.5 ± 5	∗	18.71	2.26
21		unknown		44.19	1269.5 ± 5	∗	18.90	2.33
22	1257[f]	Samalas, Indonesia[f]		44.78	1258.4 ± 5	∗	19.15	2.27
23		unknown		46.46	1228.6 ± 5	∗	19.89	2.35
24		unknown[d]		48.83	1188.8 ± 6	∗	20.90	2.41

Table 1. Continued.

No.	Year of Eruption (AD)	Volcanic Eruption Possibly Associated with Detected Event	VEI	B32 Depth[a] (m.w.e.)	B32 Age[a] (AD)	Synchronization, this work	DF01 Depth (m.w.e.)	α^b
25		unknown		50.01	1169.7 ± 6	∗	21.39	2.33
26		unknown		53.49	1111.9 ± 7			
27		unknown		53.72	1107.8 ± 7	∗	22.97	2.27
28		unknown[d]		57.77	1039.9 ± 8			
29		unknown[d]		61.53	975.9 ± 9			
30		unknown[d]		62.46	961.0 ± 10			
31		unknown[d]		76.87	718.8 ± 13			
32		unknown		78.76	686.0 ± 14	∗	34.01	2.36
33		unknown		80.94	650.0 ± 14			
34		unknown		81.71	636.8 ± 15			
35		unknown		85.08	579.5 ± 16	∗	36.69	2.33
36		unknown[d]		87.16	542.9 ± 17	∗	37.58	2.50
37		unknown		89.85	499.1 ± 17	∗	38.66	2.20
38		unknown		93.18	442.8 ± 17	∗	40.17	2.39
39		unknown		95.97	395.3 ± 18	∗	41.34	2.17
40		unknown		99.17	340.4 ± 18			
41		unknown		100.83	315.0 ± 19	∗	43.58	2.64
42		unknown[d]		103.14	279.0 ± 21	∗	44.45	2.30
43		unknown		104.93	250.9 ± 22	∗	45.23	2.30
44	230 ± 16[g]	Taupo, New Zealand[g]	6?	106.77	221.7 ± 22	∗	46.03	2.25
45		unknown[d]		108.91	187.2 ± 23	∗	46.98	

Notes: Name, location, VEI, and year, with uncertainty, of each volcanic eruption are mainly based on the work by Simkin et al. (2010) with some of the additional sources specifically shown.

[a] Depths or the year of the nssSO_4^{2-} concentration peaks, based on data (H. Oerter and R. Weller, personal communication, 2011) from the B32 core. Some of them are slightly different from those given by Traufetter et al. (2004); for example, AD 186 identified in Table 1 of Traufetter et al. (2004) has been allocated to be AD 187 (at the peak) in this study. Corresponding dating uncertainty is taken from Traufetter et al. (2004).

[b] Applied from the corresponding water-equivalent depth in the column to the left down to just before the water-equivalent depth of the next synchronized point.

[c] Based on Table 1 of Traufetter et al. (2004), but corresponding nssSO_4^{2-} spikes were not found in the data supplied by H. Oerter and R. Weller (personal communication, 2011).

[d] Different from the allocation of Traufetter et al. (2004), based on Simkin et al. (2010).

[e] Not found in Simkin et al. (2010), and adopted from Traufetter et al. (2004).

[f] Recent age determination from Lavigne et al. (2013).

[g] Different from the allocation of Traufetter et al. (2004), based on recent age determination from Simkin et al. (2010), see also Sect. 4.1.

Table 2. The part of the EDML1 chronology for AD 1170–199 correlated with the B32 chronology (Ruth et al., 2007) and the volcanic eruption dates between AD 199 and 1 (M. Severi, personal communication, 2011).

No.	B32 Age[a] (AD)	EDML1 Depth[b] (m)	EDML1 Age[b] (AD)	Error estimated for EDML1 age[c] (yr)
25	1170 ± 6	82.32	1171	± 6
26	1112 ± 7			
27	1108 ± 7			
28	1040 ± 8			
29	976 ± 9			
30	961 ± 10			
31	719 ± 13			
32	686 ± 14	117.73	694	± 13
33	650 ± 14			
34	637 ± 15			
35	580 ± 16	125.24	595	± 16
36	543 ± 17	127.65	567	± 17
37	499 ± 17	130.92	515	± 18
38	443 ± 17	134.69	460	± 19
39	395 ± 18			
40	340 ± 18			
41	315 ± 19	143.59	333	± 23
42	279 ± 21	146.22	294	± 24
43	251 ± 22	148.23	267	± 25
44	222 ± 22	150.41	235	± 25
45	187 ± 23	152.86	199	± 26
46		154.75	172	± 30
47		155.98	153	± 35
48		164.40	19	± 40
49		165.22	8	± 43

[a] Rounded off from the values given in Table 1 with errors based on Traufetter et al. (2004).

[b] Based on Ruth et al. (2007) from AD 1171 down to 199; the four additional eruption dates before AD 199 were provided by M. Severi (personal communication, 2011).

[c] Absolute errors, except for AD 1171, were estimated in this work as described in Sect. 3.2.

Table 3. Derived mean accumulation rates (MARs) at Dome Fuji based on the DFS1 and DFS2 chronologies, and DFS1-derived MARs relative to those at the DML05 drilling site.

B32 Period (AD)	MAR based on DFS1 age (mm yr^{-1})	Relative MAR	EDML1 Period (AD)	MAR based on DFS2 age (mm yr^{-1})
1884–1835	23.9	0.39	1884–1835	[a]
1835–1817	28.9	0.44	1835–1817	[a]
1817–1810	22.2	0.39	1817–1810	[a]
1810–1696	25.7	0.43	1810–1696	[a]
1696–1676	24.5	0.40	1696–1676	[a]
1676–1640	21.5	0.40	1676–1640	[a]
1640–1620	28.3	0.48	1640–1620	[a]
1620–1602	27.7	0.42	1620–1602	[a]
1602–1596	27.9	0.45	1602–1596	[a]
1596–1455	23.8	0.40	1596–1455	[a]
1455–1343	26.1	0.43	1455–1343	[a]
1343–1285	26.6	0.44	1343–1285	[a]
1285–1277	27.2	0.45	1285–1277	[a]
1277–1270	27.3	0.44	1277–1270	[a]
1270–1258	22.9	0.43	1270–1258	[a]
1258–1229	24.8	0.44	1258–1229	[a]
1229–1189	25.4	0.43	1229–1189	[a]
1189–1170	25.6	0.41	1189–1170	[a]
1170–1108	25.6	0.43	1170–694	26.5
1108–686	26.2	0.44		
686–579	25.1	0.42	694–595	27.0
579–543	24.3	0.43	595–567	31.8
543–499	24.6	0.40	567–515	20.7
499–443	26.9	0.45	515–460	27.6
443–395	24.5	0.42	460–333	26.9
395–315	28.0	0.46		
315–279	24.2	0.38	333–294	22.3
279–251	27.7	0.43	294–267	28.8
251–222	27.2	0.43	267–235	24.8
222–187	27.6	0.44	235–199	26.4
			199–172	23.8[b]
			172–153	22.3[b]
			153–19	22.7[b]
			19–8	26.5[b]

[a] The same as the corresponding MAR derived using the DFS1 chronology.

[b] Tentative derivation obtained by matching volcanic eruption dates only (see text).

Table 4. Comparison of DFS1 and DFS2 volcanic eruption dates before AD 1170 with those identified from WAIS Divide, Law Dome, and from Greenland. All eruptions are bipolar events, unless otherwise mentioned. All dates are given in AD.

Reference Volcano, Region	Sigl et al. (2013) WAIS Divide dates[a]	Plummer et al. (2012) Law Dome dates	Larsen et al. (2008) Greenland dates	This study DFS1/B32 dates	This study DFS2/EDML1 dates
Unknown	676.5/674.1	676.5–4/+1	674/675 ± 2	686 ± 14	–
Unknown	579.7	–	–	580 ± 16	595 ± 16
Unknown	565.8	566.3–5/+1	567/568 ± 2	–	567 ± 17
Unknown	531.2	530.9–5/+1	533/534 ± 2	543 ± 17	515 ± 18
Unknown	426.4	422.7–6/+2	–	443 ± 17	–
Unknown	385.8	–	–	395 ± 18	–
Unknown[b]	345.5	343.7–6/+2	–	–	–
Unknown	336.8	–	–	–	333 ± 23
Unknown	298.5	295.4–7/+3	–	279 ± 21	294 ± 24
Unknown	261.1	258.7–7/+3	–	251 ± 22	267 ± 25
Taupo, New Zealand	231.8	~ 229–7/+3	–	222 ± 22	235 ± 25
Unknown[b]	199.4	198.4–7/+3	–	187 ± 23	199 ± 26

[a] Start date in Table 1 of Sigl et al. (2013). The error estimated for this is equivalent to 3 months according to their paper.

[b] Found from the Southern Hemisphere only, according to Sigl et al. (2013).

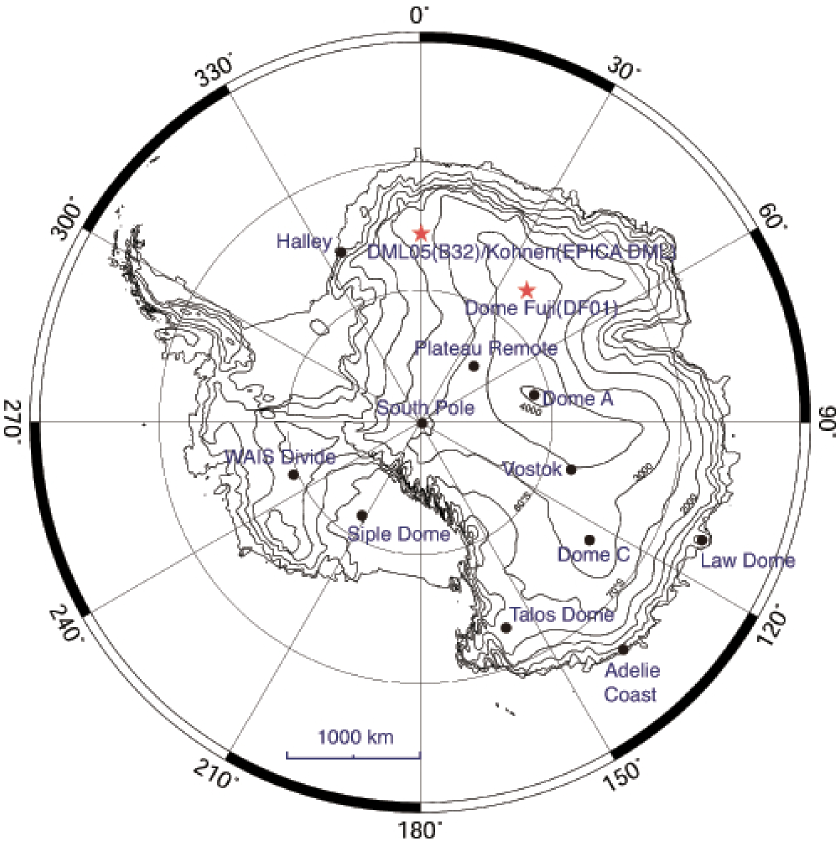

Fig. 1. Locations of drilling sites, including Dome Fuji station where the DF01 shallow core was obtained, and the DML05 site where the B32 shallow core was recovered. The DML05 point and Kohnen station, where the EPICA DML deep core was drilled, are too close together (1.7 km) to distinguish at this scale and hence are shown by a single red star.

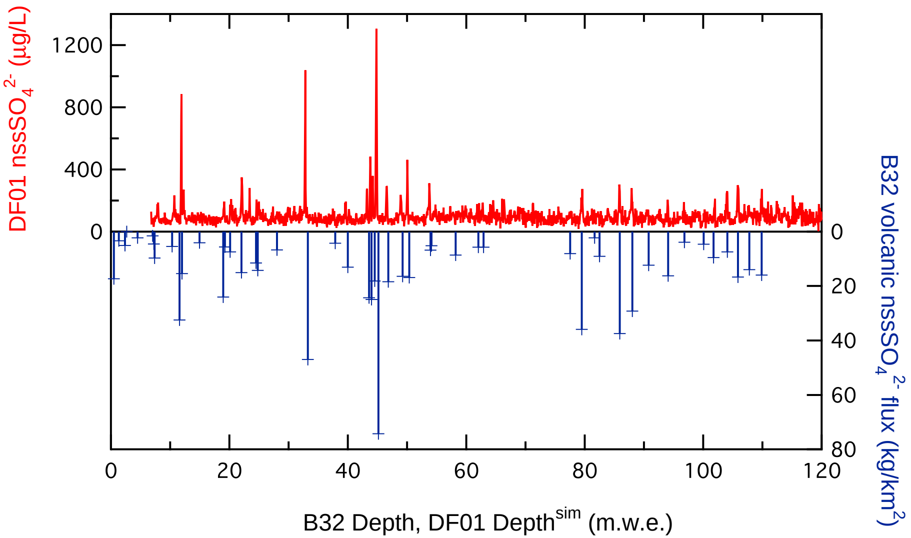

Fig. 2. Simplified overview of the synchronization between the DF01 and B32 cores. Here, the water-equivalent depth in the DF01 core (DF01 Depth^{sim}) has been simply multiplied by 2.34 over the total length to give a simple overall picture of volcanic signal correlation. The non-sea-salt sulfate data are shown on the vertical axis in relation to the water-equivalent depth values plotted on the horizontal axis. m.w.e.: meters of water equivalent.

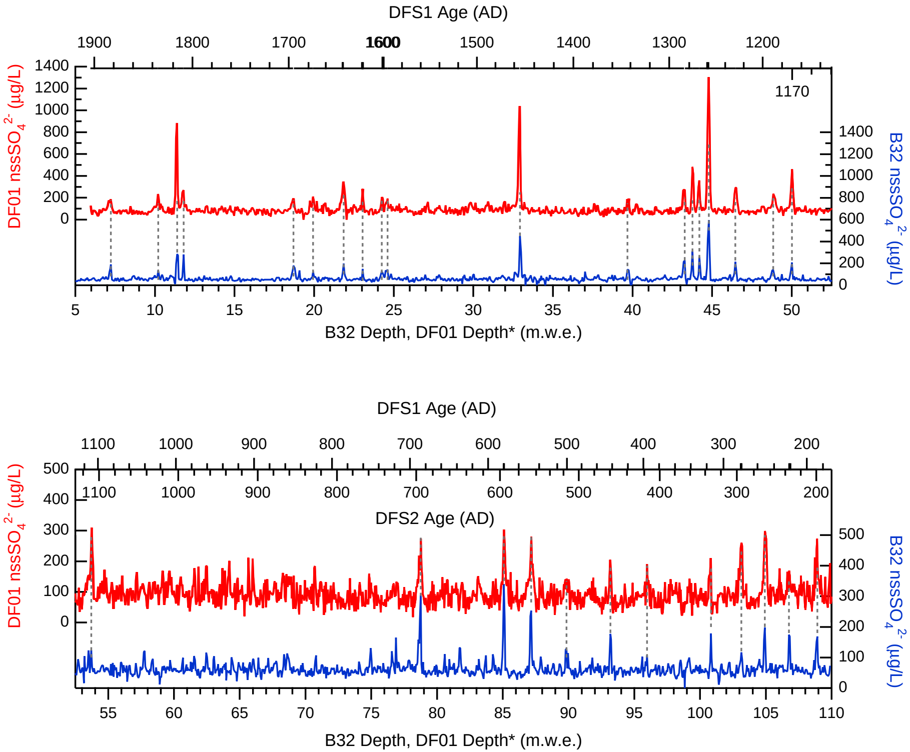

Fig. 3. Detailed volcanic signature matching between the DF01 and B32 cores, performed by using non-sea-salt sulfate records, from AD 1900 back to around AD 180. The bottom axis shows the water-equivalent depth in the B32 core, and that in the DF01 core multiplied by α, given in Table 1, in each synchronized interval. The DFS1 ages are shown above the top axes, and the DFS2 ages are shown below the top axes where they deviate from the DFS1 ages (before AD 1170). Note the difference in the scale of the ordinate between the upper and the lower panel.

Title Page
Abstract
Introduction
Conclusions
References
Tables
Figures
I◀
▶I
◀
▶
Back
Close
Full Screen / Esc
Printer-friendly Version
Interactive Discussion

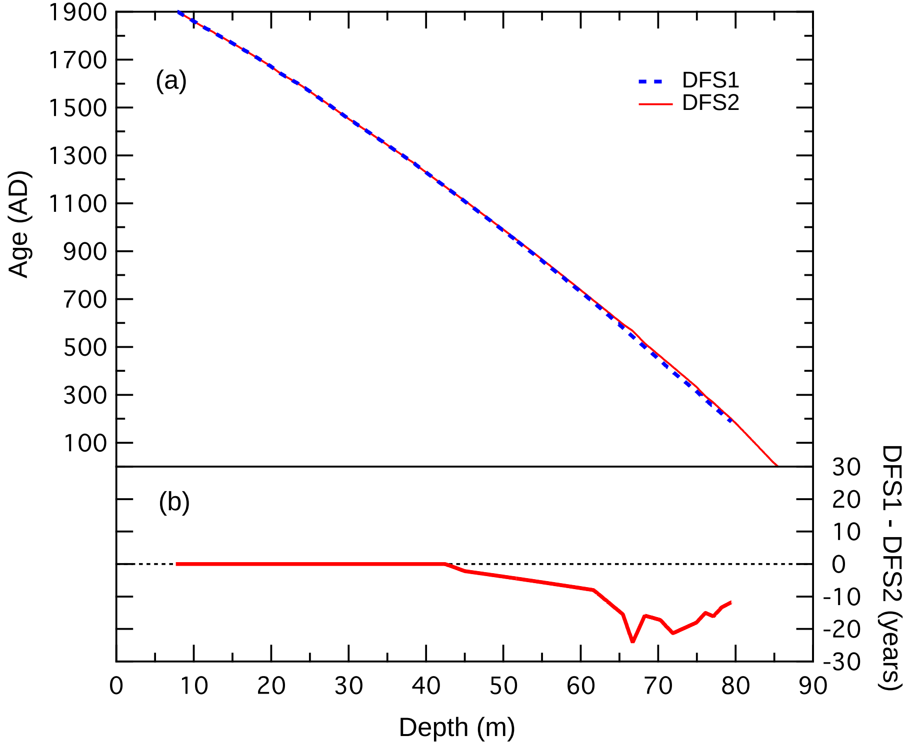

Fig. 4. Depth–age relationship in the DF01 ice core **(a)**, and the difference between the DFS1 and DFS2 time scales **(b)**.

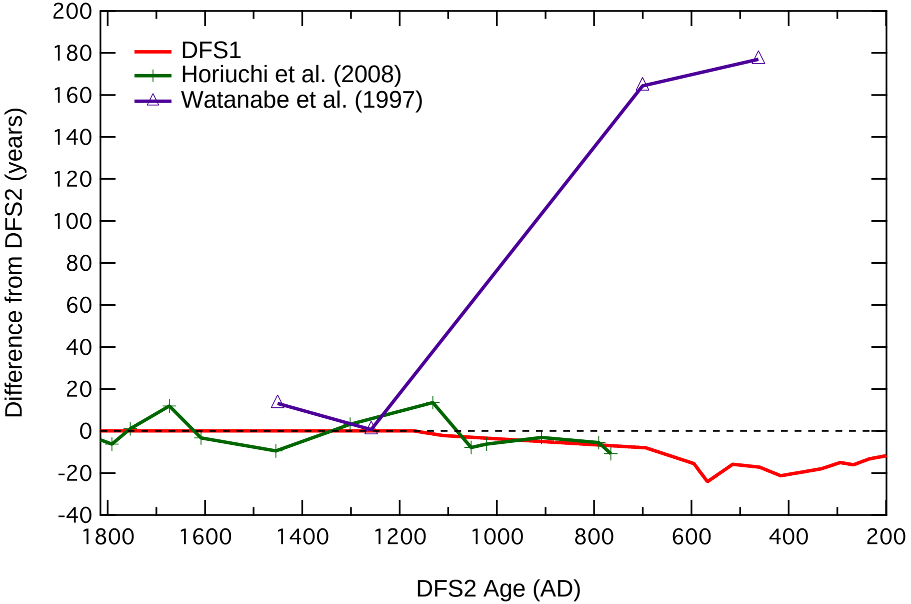

Fig. 5. Differences, relative to the DFS2 age, of the DFS1 chronology and of chronologies proposed by previous Dome Fuji shallow ice core dating studies.

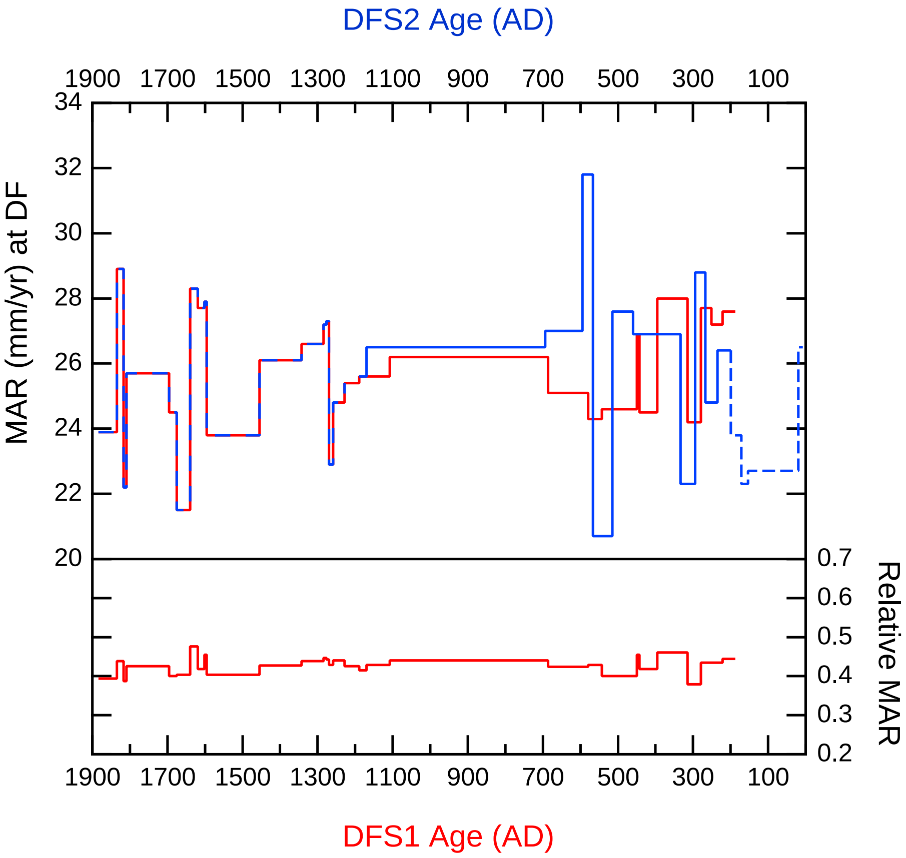

Fig. 6. Mean Accumulation Rates (MARs) at Dome Fuji based on DFS1 (red lines, bottom axis) and DFS2 (blue line, top axis) ages: absolute MARs (upper panel) and MARs relative to B32 drilling site (DML05; lower panel).